JVSTB Journal of Vacuum Science & Technology B

Classical momentum gap for electron transport in vacuum and consequences for space charge in thermionic converters with a grid electrode

Amir H. Khoshaman and Alireza Nojeh

Citation: Journal of Vacuum Science & Technology B **34**, 040610 (2016); doi: 10.1116/1.4958801
View online: http://dx.doi.org/10.1116/1.4958801
View Table of Contents: http://scitation.aip.org/content/avs/journal/jvstb/34/4?ver=pdfcov
Published by the AVS: Science & Technology of Materials, Interfaces, and Processing

Classical momentum gap for electron transport in vacuum and consequences for space charge in thermionic converters with a grid electrode

Amir H. Khoshaman[a] and Alireza Nojeh[b]
Department of Electrical and Computer Engineering, University of British Columbia, Vancouver, British Columbia V6T 1Z4, Canada

(Received 25 April 2016; accepted 29 June 2016; published 21 July 2016)

Quantum mechanics tells us that the bound states of a potential well are quantized—a phenomenon that is easily understandable based on wave properties and resonance. Here, the authors demonstrate a classical mechanism for the formation of a momentum gap in the phase space of electrons traveling as particles in a potential well in vacuum. This effect is caused by the reflection of electrons from at least two potential maxima, which may, for instance, exist due to space-charge distribution in a triode configuration. This gap plays a critical role in space-charge-mitigated electron transport in vacuum, such as in a thermionic energy converter with a positively biased grid, where it is shown that the current density can be increased by 1–3 orders of magnitude depending on the severity of space charge in the absence of the grid. © *2016 American Vacuum Society*.
[http://dx.doi.org/10.1116/1.4958801]

I. INTRODUCTION

Energy gaps and quantization of momentum states are commonly associated with quantum mechanical or wave phenomena arising in nanoscale potential wells. Here, we show that momentum gaps could arise in the phase space of electrons traveling in classical potential wells (where the dimensions are large enough that quantization due to the wave nature of the electrons is negligible) due to purely classical effects.

Imagine that a stream of electrons with a wide range of positive initial velocities is fired (from the left hand side) at the potential (motive) profile depicted in Fig. 1(a) and is fully collected once it reaches the right hand side. For the moment, the interactions among the electrons are neglected; they will be subsequently included in the more detailed discussion below. On their path, electrons face two potential barriers in the interelectrode region, and a potential well between those. If the height of the second barrier is higher than that of the first one, the reflection of the electrons from these two barriers will lead to an interesting phenomenon, whereby certain momenta will not be permissible in the potential well between points 2 and 5. The emergence of this behavior can be understood by considering that only electrons with initial kinetic energies above the first barrier (point 2) can enter the well. At any subsequent point in the well, these forward-moving electrons will have velocities greater than a certain value $v_2(x)$, which depends on the local potential. These constitute the positive, semi-infinite shaded band on the corresponding velocity distribution graph on Fig. 1(a). Of these electrons, those with a kinetic energy below the second barrier will be reflected and constitute the negative, finite shaded band on the velocity distribution graph. This leads to a position-dependent momentum gap centered around zero, as can be seen on the distribution. In the regions between points 1 and 2, and between points 5 and 6, which are outside the potential well, this gap disappears as the electrons, both forward-moving and those reflected from the barriers, can have velocities all the way down to zero. Similarly, in the region between points 6 and 7, electrons will have only forward momentum and there will be no gap. Note that, if the first potential barrier (point 2) is taller than the second one (point 6), this phenomenon will not occur, since in this case only electrons with initial kinetic energies higher than the tallest barrier will enter the potential well and they will not be reflected from the second barrier.

It is interesting to observe that this momentum gap emerges due to the existence of both forward-moving and reflected electrons in the system. This is reminiscent of the quantization of momentum in a quantum well, which could be regarded as being the result of interference of forward-travelling and backward-travelling waves. Nevertheless, the two are fundamentally different effects.

II. THEORY AND MODEL

We now turn to a detailed analysis of the problem and discuss the profound role of this momentum gap on electron transport. The potential well portrayed in Fig. 1(a) can be generated by the device configuration depicted in Fig. 1(b). Electrons with various kinetic energies are released from a source electrode (the emitter), pass through a potential well and are collected by another electrode (the collector). The potential well can be formed by the introduction of one or several auxiliary electrodes, namely, grids [Fig. 1(b)]; the motive may also be lowered by other means, such as the presence of positive ions in the system or the use of negative electron affinity materials.[1] One way to create a distribution of initial velocities at the emitter surface is the ejection of electrons from a hot electrode due to thermionic emission. In the steady state, such electrons assume a hemi-Maxwellian (HM) distribution at the emitter if the motive of the point

[a]Electronic mail: akhosham@ece.ubc.ca
[b]Electronic mail: anojeh@ece.ubc.ca

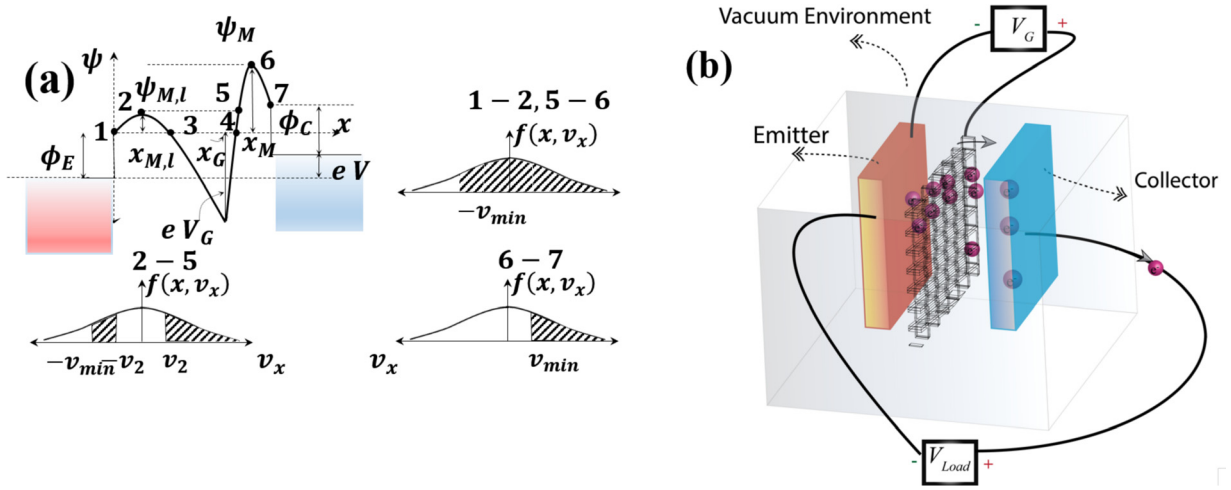

FIG. 1. (Color online) (a) Potential (ψ) or motive profile of a potential well as a function of distance, x, and the resulting velocity distribution functions, $f(x, v_x)$, in different regions. (b) Schematic of a vacuum device comprising an emitter, a collector, and an ancillary electrode (grid) that allows the transport of electrons through the classical potential well. The potential well depicted in (a) is due to the external applied fields and the interaction between the electrons in the interelectrode region. Note that the value of the momentum gap depends on position, with its maximum value occurring at the position of the grid (where motive is at its minimum).

just outside the collector lies below that just outside the emitter. In a more general sense, electrons assume an HM distribution at the point of maximum motive in the interelectrode region.

Here, we show how these effects can be quantified by solving the Vlasov equation. The electrodes are assumed to be infinitely large in lateral dimensions, so that a one-dimensional (1D) Vlasov equation can be used. (We expect that the momentum gap will leave its mark in the 3D case as well, although the analysis would be more complex in that case.) The virtue of using the Vlasov equation is that the electron–electron interactions are automatically included (albeit in a mean-field manner) when solved self-consistently with the Poisson equation, leading to correct results in the steady state.

In this case, the steady-state collisionless Vlasov equation can be written as $v_x(\partial f(x,v_x)/\partial x) - (1/m)(d\psi(x)/dx)(\partial f(x,v_x)/\partial v_x) = 0$,[2] where x denotes the direction normal to the emitter's surface, $\psi(x)$ represents electron motive (in this case, electric potential energy), v_x is the electron velocity along the direction of propagation, $f(x,v_x)$ is the velocity distribution function,[3] and m is the electron mass. The solution to this equation can assume the form of any arbitrary function of an integral of motion,[4] such as the energy of an electron, $(1/2)mv^2 + \psi(x)$. The exact solution can be obtained by applying the proper boundary condition [Fig. 1(a)], i.e., electrons having an HM distribution at the point of maximum motive, (x_M, ψ_M), which can be written as

$$f(x_M, v) = 2\, n(x_M) v_{th}^{-3} \exp\left(-\beta\left(\frac{1}{2}mv^2 + \psi(x_M) - \psi_M\right)\right) \times \Theta(v_x), \tag{1}$$

where $\psi(x_M) \equiv \psi_M$, v_{th} is the average thermal velocity of the HM distribution, $(2\pi/m\beta)^{1/2}$, Θ is the unit step function, and $\beta = 1/k_B T_E$, where k_B is the Boltzmann constant and T_E is the temperature of the emitter. Depending on the actual voltage and current values in the device, a total of eight possible motive configurations, leading to different distribution functions, could arise in the presence of an emitter, a collector, and an ancillary electrode. A case that satisfies the two aforementioned conditions required for the emergence of velocity gaps is depicted in Fig. 1(a). Electrons on the right hand side of the maximum motive (points 6–7) can only move unidirectionally since they had enough kinetic energy to surmount the motive barrier, with a minimum velocity $v_{\min} = (2\gamma/\beta m)^{\frac{1}{2}}$, where $\gamma \equiv \beta(\psi_M - \psi(x))$. Therefore, for such points

$$f(x, v) = 2\, n(x_M) v_{th}^{-3} \exp\left(-\beta\left(\frac{1}{2}mv^2 + \psi(x) - \psi_M\right)\right) \times \Theta(v_x - v_{\min}). \tag{2}$$

After integration, this results in the electron density $n(x) = n(x_M)\exp(\gamma)(1 - \mathrm{erf}\gamma^{1/2})$.

In regions where electrons face a barrier (or barriers) only in the forward direction, that is, between points 1 and 2, and between points 5 and 6, they move bidirectionally since those without sufficient energy to overcome all the barriers are scattered and fully reverse their direction, resulting in negative velocities. In such cases, we have

$$f(x, v) = 2\, n(x_M) v_{th}^{-3} \exp\left(-\beta\left(\frac{1}{2}mv^2 + \psi(x) - \psi_M\right)\right) \times \Theta(v_x + v_{\min}), \tag{3}$$

and $n(x) = n(x_M)\exp(\gamma)(1 + \mathrm{erf}\gamma^{1/2})$. A special behavior emerges at points between the two peaks $\psi_{M,l}$ and ψ_M, with motives smaller than $\psi_{M,l}$ (points 2–5). In such cases, the first, smaller peak blocks the electrons with initial kinetic energies smaller than $\psi_{M,l}$. This results in

$$f(x,v) = 2\,n(x_M)v_{th}^{-3}\exp\left(-\beta\left(\frac{1}{2}mv^2+\psi(x)-\psi_M\right)\right) \times\left\{\Theta(v_x+v_{\min})-\Theta(v_x+v_2)+\Theta(v_x-v_2)\right\}, \tag{4}$$

where $v_2 = (2\gamma_l/\beta m)^{1/2}$ and $\gamma_l \equiv \beta(\psi_{M,l}-\psi(x))$, according to Fig. 1(a). The velocity gap centered around zero is due to the absence of electrons with initial kinetic energies between 0 and $\psi_{M,l}$, whereas the absence of velocities less negative than $-v_{\min}$ is because any electron with initial kinetic energy higher than the tallest peak ($\psi_{M,l}$) will not be reflected. This leads to the distinct, negative velocity band seen on Fig. 1(a) in the region between points 2 and 5. Integration of the distribution function results in

$$n(x) = n(x_M)\exp(\gamma)(1-2\,\mathrm{erf}\gamma_l^{1/2}+\mathrm{erf}\gamma^{1/2}). \tag{5}$$

Electron densities at high values of γ and γ_l were calculated by using an asymptotic expansion of the error function[5] or numerically integrating the velocity distribution function using the method of global adaptive quadrature.[6]

It is noted that the momentum gaps depend on the position and the width of the gap at each point in the region between the points 2 and 5 depends on the local value of the motive. More specifically, points 2 and 5 are the boundary points at which the momentum gaps start to emerge, and the momentum gap has its maximum value at the position of the grid (which has the most negative motive).

If the electrochemical potential of the collector is above that of the emitter, this device operates in the power generation mode and is referred to as a thermionic energy converter or thermoelectronic energy converter (TEC). TECs are the perfect vehicle to investigate the velocity/momentum gap phenomenon presented above due to three reasons. First, the thermal emission of the electrons from the hot electrodes furnishes the wide range of initial kinetic energies needed. Second, these devices generally operate at low biases, making the space-charge effect prominent; since the collector is at a higher electrochemical potential, depending on the workfunctions and the operating conditions, it is more likely to be in retarding mode (where the point just outside the collector has a higher motive than the point just outside the emitter). Indeed, a reason that this effect has not been reported in the past could be that most vacuum electronic devices normally operate deep in the accelerating mode. Last, it is expected that the usage of a grid can significantly improve the current density of these devices,[7,8] and the observed velocity/momentum gap can play a fundamental role in this space-charge mitigation strategy. TECs are gaining popularity, partly because nanotechnology has opened up new avenues for addressing some of their long-standing challenges.[1,8–12] A survey of some of the advances in thermionic conversion enabled by nanotechnology is given in Ref. 13. As a case study, we now apply the electron velocity distributions discussed above to the steady state behavior of a TEC comprising a grid and demonstrate that the application of sufficiently positive grid biases can significantly improve its current density.

The thermionic emission current from the electrodes is evaluated from the Richardson-Dushman equation, $J_{sat} = AT_E^2\exp(-\phi_E/k_BT)$, where J_{sat} is the saturation current density, ϕ is the workfunction, and $A = 1.202\times10^6\,\mathrm{A\,m^{-2}K^{-2}}$ is the Richardson constant.[14] This equation is used as the boundary condition to the Vlasov equation as the incident flux of forward-going electrons at the emitter. It is assumed that electrons start off from the emitter and are fully absorbed upon arrival at the collector.

The electron densities obtained from the Vlasov equation are substituted in the Poisson equation, $(d^2\psi(x)/dx^2) = -(e^2/\epsilon_0)n(x)$, subject to the boundary conditions $\psi(0)=0$, $\psi(x_G)=eV_G$, and $\psi(d)=eV_{int}$, where e is the electron charge, ϵ_0 is the permittivity of vacuum, and V_{int} is the internal motive difference between collector and emitter. When the workfunctions are equal, the magnitude of the internal motive difference is equal to the difference between the electrochemical potentials of the emitter and collector, V_{Load}. However, in the more general case, where the workfunctions are not equal, the value of the internal voltage difference is equal to $V_{\mathrm{Load}} - (\phi_E-\phi_C)/e$. It is assumed that the grid's length scale is finer than the Debye length of the electron gas (typically 10–500 μm in TECs). Under this condition, the plane of the grid (including the holes) can be considered to be an equipotential surface and thus the motive at the gate position can be set equal to eV_G, where V_G is the grid bias with respect to the emitter. The Poisson equation is solved recursively with the Vlasov equation using the strategy portrayed in Ref. 15, where we have also presented an algorithm to ensure convergence.

III. RESULTS AND DISCUSSION

The motive and electron density distributions of a TEC are depicted in Fig. 2 (see the figure caption for the device parameters used). The position of the grid is chosen such that the tallest motive peak occurs after the grid, in accordance with the conditions necessary to generate the momentum gaps.

The velocity gaps are indispensable to the problem; in their absence, the system becomes unstable and therefore not physically realizable. This can be understood by the following argument. For this transport system to be physically possible, there needs to be a negative feedback mechanism between the concentration of the electrons and the motive profile that is generated due to the presence of these electrons and the external potentials. This requirement is rooted in the fact that electrons are only ejected from the emitter, and henceforth, their concentration needs to decrease in the region between point 2 and the grid (Fig. 2); otherwise, they are being accumulated inside the well. However, this cannot occur in steady state. This argument is supported mathematically by noting that the electron density function in the region between point 2 and the grid [Eq. (5)] in Fig. 1(a) is a decreasing function of distance, except for when the value of γ_l plunges below 0.4769. However, this does not lead to instability since the local barrier height on the left will increase due to accumulation of charges in the well, which will in turn increase the value of γ_l, rendering the system stable.

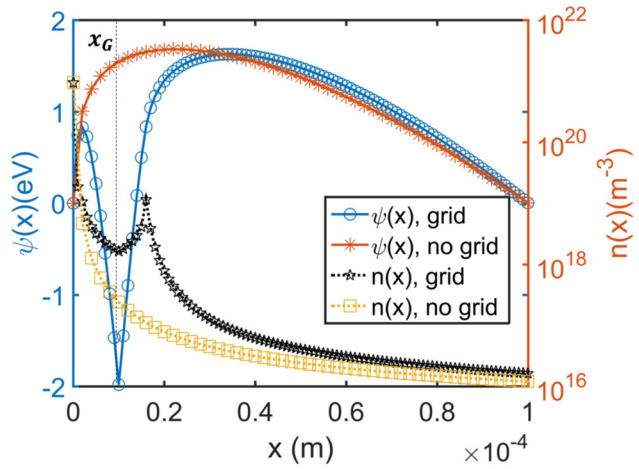

FIG. 2. (Color online) Motive profile and the electron density of a TEC with $\phi_E = \phi_C = 2.5\,\text{eV}$, $T_E = 2200\,\text{K}$, $d = 100\,\mu\text{m}$, $x_G = 10\,\mu\text{m}$, and $V = 0\,\text{V}$. Also shown are the potential profile and the electron density for the same TEC, but in the absence of a grid. As detailed in the main text, the overall effect is a total reduction in the maximum motive barrier.

The motive and the electron density versus distance are depicted in Figs. 3(a) and 3(b) for several applied grid voltages for a TEC with the parameters given in the figure caption; the maximum motive as a function of the grid voltage is plotted in Fig. 3(c). It is interesting to note that increasing the grid voltage impacts the device performance in two opposing ways: the overall electron density is increased by increasing the grid voltage according to Figs. 2 and 3(b), since more electrons are allowed to be in the interelectrode region compared to the case where no grid is present. This is due to the presence of higher potential energy differences, leading to a larger spectrum of kinetic energies and velocities. Therefore, the higher number of electrons in the interelectrode region increases the space charge potential. The other effect is that the motive boundary (on the grid) is shifted downward due to the negative motive. Mathematically, the first effect is due to the Vlasov equation, whereas the second one is due to the boundary conditions to the Poisson equation. The interplay between these factors leads to an overall reduction in the maximum motive [Figs. 2 and 3(c)] and hence an increase in the current density.

The outcome is that the solution to the Poisson equation has a smaller peak compared with the case where no grid is present

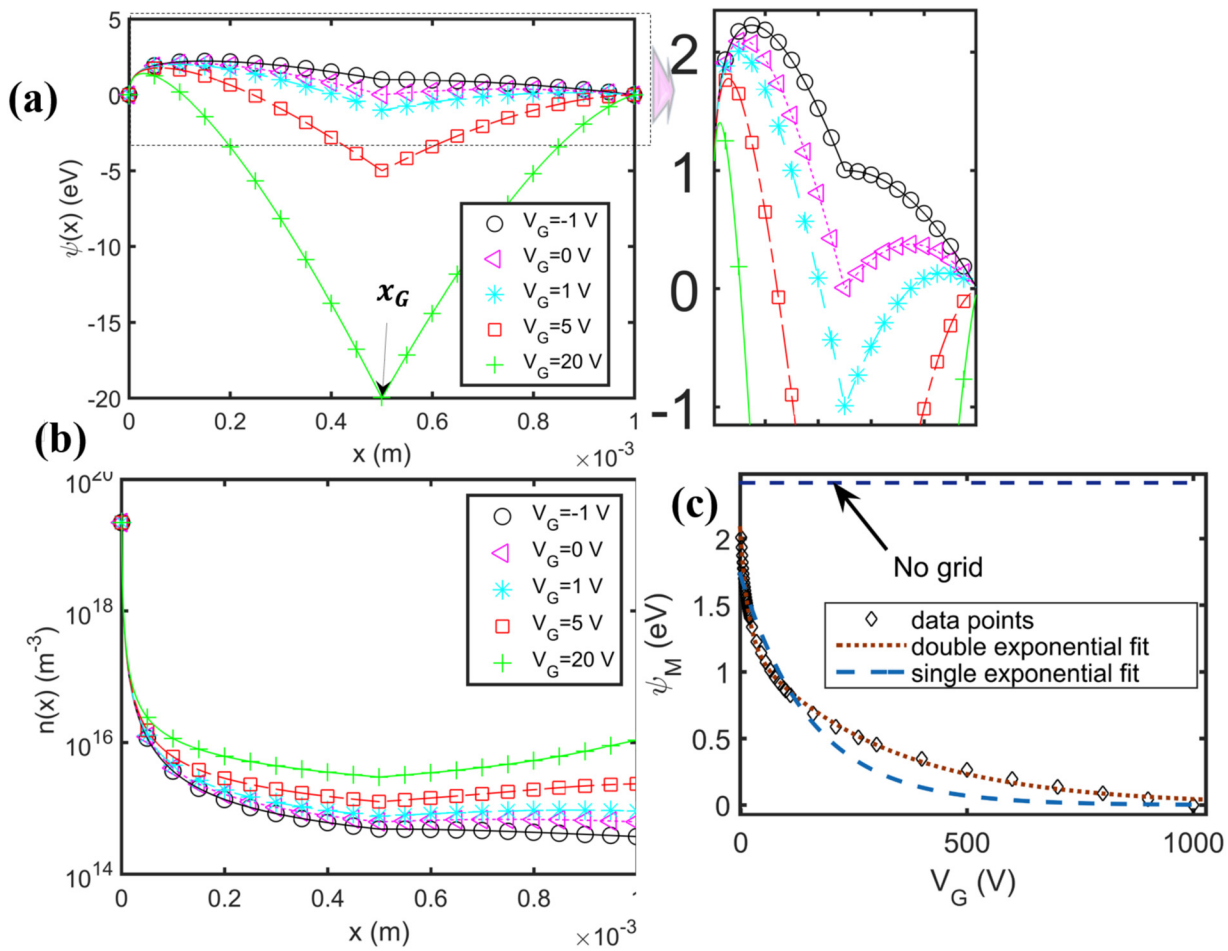

FIG. 3. (Color online) (a) Motive as a function of position for a TEC with $\phi_E = \phi_C = 4.5\,\text{eV}$, $T_E = 3000\,\text{K}$, $d = 1\,\text{mm}$, and $x_G = 500\,\mu\text{m}$ for different values of the grid bias. (b) The electron density as a function of position for different gate biases. (c) The maximum motive, ψ_M, as a function of the grid bias. The computed data can be fit by a double exponential function, $\psi_M = a\exp(bV_G) + c\exp(dV_G)$, where $a = 0.03798, b = -3.983$, $c = 1.075$, and $d = -0.2363$ with RMSE $= 0.01705$.

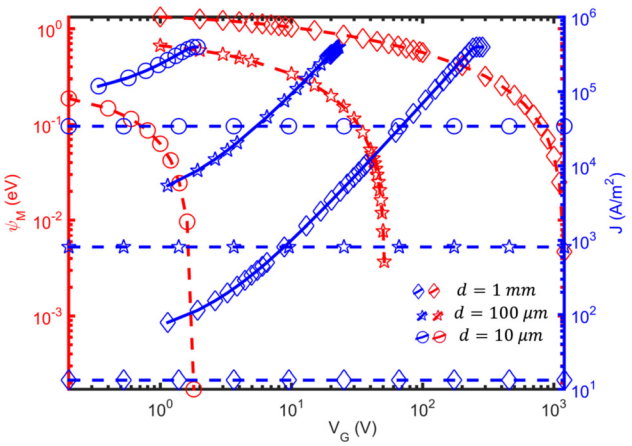

FIG. 4. (Color online) Maximum motive (descending curves) and the current density (ascending curves) as a function of the grid bias for different values of d. The current densities in the absence of the grid are plotted as dashed lines. The parameters of the TEC are $\phi_E = \phi_C = 2.5\,\text{eV}$, $T_E = 1800\,\text{K}$, and $x_G = d/2$.

[Figs. 2, 3(a), and 3(c)]. The presence of these two effects can be demonstrated in Fig. 3(c), where it is noted that a single exponential curve cannot capture the trend of changes of ψ_M, and that a biexponential function is necessary for this purpose. It is also noted from Fig. 3(c) that even setting $V_G = 0$ is more favorable than not having a gate at all.

The developed model can be used to calculate the value of the grid bias necessary to obtain a certain amount of current density or motive barrier. The results are depicted in Fig. 4 for a TEC (see the device parameters in the figure caption) at different values of d. It is observed that at smaller values of d—applicable to most emerging TECs—smaller values of grid bias, on the order of several volts, can diminish the space charge effect and improve the output power density by an order of magnitude. At higher distances, a higher grid bias is needed according to Fig. 4 in order to eliminate the space charge effect, since more electrons inhabit the interelectrode region.

Reducing the workfunction of the emitter results in an exponential increase in current, leading to the amplification of the space charge. Increasing the emitter temperature also has a similar effect. Therefore, smaller workfunctions with a smaller emitter temperature were used to obtain the results shown in Fig. 4 compared to Fig. 3. Similarly, in order to demonstrate the influence of the momentum gap on the operation of the TEC in Fig. 2, a higher temperature than that for Fig. 4 was chosen, so as to compound the space charge effect.

The results presented so far do not take into account possible electron loss to the grid. This loss can be easily included in the model by multiplying the current density at each iteration level by $(1 - l)$, where l represents the loss fraction of the grid. This reduced current density leads to a lower $n(x_M)$ and therefore lower space charge at the expense of power loss through the grid. If a bias of 2 V is applied to the grid, the geometric loss corresponds to ~4% loss in the total output power if space charge is completely eliminated. On the other hand, if higher voltages are applied, it is necessary to reduce the grid loss further to improve the overall efficiency. Meir *et al.* reported that, by applying a longitudinal magnetic field, the electron transparency of a grid can be enhanced to its geometrical transparency (which could be as high as 98%);[8] by using nanomaterials such as graphene, it is also possible to achieve high transparency.[16–19] The presented model also neglects the electronic structure of the grid metal and its impact on the energy dependence of the absorption/reflection/transmission coefficients of the impinging electrons; for cases where this might become important, such as in atomically thin grids, the model needs to be modified to incorporate this energy-dependent behavior.

IV. SUMMARY

We showed that momentum gaps could arise in the phase-space of electrons traveling under certain conditions in vacuum. The transport model for this phenomenon was developed and employed to analyze the performance of thermionic energy converters in the presence of grids. It was further demonstrated that the application of positive voltages to the grid can significantly mitigate the space charge effect.

ACKNOWLEDGMENTS

The authors thank George A. Sawatzky, Jochen Mannhart and R. Fabian Pease for fruitful discussions. Financial support was provided by the Natural Sciences and Engineering Research Council of Canada (SPG-P 478867) and the Peter Wall Institute for Advanced Studies. Amir H. Khoshaman also thanks the University of British Columbia for additional support.

[1]J. R. Smith, G. L. Bilbro, and R. J. Nemanich, J. Vac. Sci. Technol., B **27**, 1132 (2009).
[2]F. F. Chen, *Introduction to Plasma Physics and Controlled Fusion. Volume 1, Plasma Physics*, 2nd ed. (Springer, New York, 2006).
[3]J. A. Bittencourt, *Fundamentals of Plasma Physics* (Springer, New York, 2004).
[4]R. C. Tolman, *The Principles of Statistical Mechanics* (Oxford University, London, 1938).
[5]G. B. Arfken and H. J. Weber, *Mathematical Methods for Physicists, Seventh Edition: A Comprehensive Guide*, 7 ed. (Academic, Amsterdam, Boston, 2012).
[6]W. M. McKeeman, Commun. ACM **5**, 604 (1962).
[7]G. N. Hatsopoulos and E. P. Gyftopoulos, *Thermionic Energy Conversion* (MIT, Cambridge, 1973), Vol. 1.
[8]S. Meir, C. Stephanos, T. H. Geballe, and J. Mannhart, J. Renewable Sustain. Energy **5**, 43127 (2013).
[9]T. L. Westover, A. D. Franklin, B. A. Cola, T. S. Fisher, and R. G. Reifenberger, J. Vac. Sci. Technol., B **28**, 423 (2010).
[10]V. S. Robinson, T. S. Fisher, J. A. Michel, and C. M. Lukehart, Appl. Phys. Lett. **87**, 61501 (2005).
[11]A. H. Khoshaman, H. D. E. Fan, A. T. Koch, N. H. Leung, and A. Nojeh, in *2014 27th International Vaccum Nanoelectronics Conference, IVNC* (2014), pp. 59–60.
[12]A. H. Khoshaman, A. T. Koch, M. Chang, H. D. E. Fan, M. V. Moghaddam, and A. Nojeh, IEEE Trans. Nanotechnol. **14**, 624 (2015).
[13]A. Khoshaman, H. D. E. Fan, A. Koch, G. Sawatzky, and A. Nojeh, IEEE Nanotechnol. Mag. **8**, 4 (2014).
[14]C. R. Crowell, Solid-State Electron. **8**, 395 (1965).
[15]A. H. Khoshaman and A. Nojeh, J. Appl. Phys. **119**, 44902 (2016).
[16]S. Srisonphan, M. Kim, and H. K. Kim, Sci. Rep. **4**, 3764 (2014).
[17]J.-A. Yan, J. A. Driscoll, B. K. Wyatt, K. Varga, and S. T. Pantelides, Phys. Rev. B **84**, 224117 (2011).
[18]C. Li *et al.*, Adv. Funct. Mater. **24**, 1218 (2014).
[19]M. Kim and H. K. Kim, J. Appl. Phys. **118**, 104504 (2015).